ECASIA special issue paper

SURFACE and INTERFACE ANALYSIS

Received: 31 August 2011 Revised: 28 October 2011 Accepted: 7 November 2011 Published online in Wiley Online Library: 2 February 2012

(wileyonlinelibrary.com) DOI 10.1002/sia.4803

Analytical methodologies for the investigation of soil-induced degradation of Cu-based archaeological artefacts†

A. Mezzi,[a]* T. de Caro,[a] C. Riccucci,[a] E. I. Parisi,[a] F. Faraldi,[b] P. Vassiliou[c] and S. Grassini[b]

Archaeological bronze artefacts are covered with corrosion products, that is, the *patinas*, whose nature depends on different degradation processes occurring during long-term burial. As a consequence of the corrosion phenomenon, surfaces of archaeological metal objects are composed of a complex structure. By means of the combined use of different analytical techniques such as XPS, scanning electron microscopy combined with energy dispersive X-ray spectroscopy, optical microscopy and X-ray diffraction, some typical *patinas* grown on Roman and Punic archaeological bronze artefacts have been studied in details by selecting a suitable methodological approach to acquire micro-chemical, morphological and structural information. The XPS measurements of Cu 2p, Cu LMM and valence band spectra of archaeological objects and reference samples such as $CuCl_2$, CuCl, $Cu_2Cl(OH)_3$, Cu_2O and CuO allowed us to identify the different copper oxidation states and crystallographic phases present in a *patina*. Moreover, the XPS elemental concentration depth profiles have yielded information about the stratified outermost layers and the occurrence of the migration phenomenon from bulk to surface due to selective corrosion processes. These pieces of information compared with those achieved via scanning electron microscopy combined with energy dispersive X-ray spectroscopy, optical microscopy and X-ray diffraction reveal the complex chemistry and morphology of the *patina*, highlighting also the correlation between *patina* and burial context. Copyright © 2012 John Wiley & Sons, Ltd.

Keywords: bronze; corrosion; archaeological artefacts; XPS; SEM–EDS; XRD

Introduction

Archaeological artefacts are often the witness of the amazing skill used to produce common use objects and works of art that disclose the high level of empirical technological competence and the sophisticated feeling for shape and chromatic effect.[1] Archaeological artefacts crossed many centuries and have been found in excavations of historic sites where their nature and appearance could have been modified by degradation processes occurred during long-term burial.[2] Concerning ancient metals, multiple factors can play a role in determining the extent and nature of degradation phenomena; the latter can be classified as endogenous (nature and metallurgical features of alloy, manufacturing technology used to produce and to shape the object) and exogenous factors (soil features such as porosity, humidity, conductivity, pH, presence of anions, etc.).[2,3] Other factors can be the recent anthropogenic factors such as acid rain, use of fertilisers and wrong exhibition conditions that could induce degradation phenomena such as the self-sustaining process romantically defined as 'bronze disease', which disfigures and even destroys the object.[2,4–8] All this information must be acquired to identify tailored conservation strategies by determining chemical composition and metallurgical features of the metal objects, nature and structure of corrosion products, burial soil characteristics and degradation agents and mechanisms. Hence, the corrosion phenomenon in archaeological metal artefacts can be understood by applying a multidisciplinary approach able to characterise the chemistry and the structure of the corrosion products.

During the past decades, many studies have been carried out[2,3,5–8] to investigate chemical the composition and structure of the archaeological bronze corrosion products by using different analytical techniques. Among these, surface analytical techniques such as XPS, scanning electron microscopy combined with energy dispersive spectrometry (SEM–EDS), X-ray diffraction (XRD) and optical microscopy (OM) can play an important role for the characterisation of ancient metal objects.

According to this multidisciplinary approach, in the present work, the surface of some bronze archaeological objects characterised by typical corrosion products have been studied in details by means of the combined use of XPS, SEM–EDS, OM and XRD. The experiments were performed to confirm the high versatility and the analytical ability of these non-invasive or micro-destructive investigation techniques in providing reliable and useful information

* *Correspondence to: A. Mezzi, ISMN-CNR, Monterotondo Stazione, Rome 00015, Italy. E-mail: alessio.mezzi@ismn.cnr.it*

† *Paper published as part of the ECASIA 2011 special issue.*

a *Istituto per lo Studio dei Materiali Nanostrutturati-CNR, Area della Ricerca RM1-Montelibretti, via Salaria Km 29.3, 00015 Monterotondo, Rome, Italy*

b *Dipartimento Scienza dei Materiali ed Ingegneria Chimica, Politecnico di Torino, Corso Duca degli Abruzzi 24, 10129 Torino, Italy*

c *National Technical University of Athens, Iroon Polytechneiou 9, 15780, Athens, Greece*

able to contribute to ensure a long-term chemical–physical stability of archaeological bronze artefacts.

Experimental

Archaeological bronze artefacts have been analysed in as-received condition before preventive conservation and restoration procedures.

X-ray diffraction patterns were recorded directly both on fragments or objects and on a small amount of *patina* scraped from the surface (50–100 mg). Diffraction patterns were recorded by a Siemens 5000 X-ray powder diffractometer (Germany) with Ni-filtered Cu Kα radiation ($\lambda = 0.154056$ nm) using the following experimental conditions: 2θ angular values between 10° and 80° in additive mode, a step size of 0.05° 2θ and a sampling time of 20 s. X-ray diffraction patterns were analysed by using electronic databases.

Optical microscopy investigation was carried out by using a Leica MLF III microscope equipped with a digital camera.

Both FE-SEM–EDS and SEM–EDS characterisations were carried out by a Cambridge 360 scanning electron microscope (SEM) Carl Zeiss (Germany), equipped with a LaB_6 filament; a high brilliance LEO 1530 field emission scanning electron microscope (FE-SEM) apparatus, Oxford Instr. (UK), equipped with an energy dispersive X-ray spectrometer (EDS) INCA 250 and INCA 450, respectively; and a four-sector backscattered electron detector (BSD). SEM images were recorded both in the secondary electron image (SEI) and backscattered image modes at an acceleration voltage of 20 kV. FE-SEM images were recorded both in the SEI and BSD modes at different acceleration voltage ranging from 3 to 20 kV. Samples were coated with a thin layer of carbon or chromium to avoid charging effects. The carbon coating was deposited by using an Emitech sputter coater K550 unit (Italy), a K 250 carbon coating attachment and a carbon cord at a pressure of 1×10^{-2} mbar to produce a carbon film with a constant thickness of about 3.0 nm.

X-ray photoelectron spectroscopy measurements were performed in an ESCALAB MkII (UK) (VG Scientific) spectrometer, equipped with a standard Al Kα excitation source and a 5-channeltron detection system. The spectra were collected at 20 eV constant pass energy and a base pressure in the analysis chamber of 10^{-8} Pa, which was increased up to 10^{-5} Pa during depth profiling. The energy of the Ar^+ ion gun was set to 2.0 keV, and the sample current density was set to about 2 μA/cm^2. A selected area of the sample was sputtered by using a Au mask with a hole of 10 mm in diameter. For the surface to be preserved during measurements, the sample holder was cooled with liquid N_2[9] avoiding the reduction effects due to X-ray and Ar^+ ion flux. The binding energy (BE) scale was calibrated by measuring the reference peaks of Au $4f_{7/2}$ (84.0 eV) from the mask and C 1 s (285.0 eV) from the surface contamination. Registered spectra were processed by the CasaXPS v. 2.2.84 software (Neal Fairley, Casa software), using a peak-fitting routine with symmetrical Gaussian–Lorentzian functions. Background intensity was subtracted from the photoelectron spectra using the Shirley method. More experimental details of XPS have been reported elsewhere.[10,11]

Results and discussion

Table 1 shows the chemical composition of bronze archaeological artefacts expressed as weight percent (hereafter wt%). As it can be noted, copper is the main component of archaeological alloys[2,12] that can be assigned to the class of bronzes where tin is present in different amounts ranging from 3.4 to 10.4 wt% and lead from 0.6 to 3.1 wt%.

Table 1. Content of Cu, Sn, Zn, Pb and Fe (expressed as weight percent, hereafter wt%) present in the matrix of the archaeological bronzes Ca-C1, Ro-C3 and N-1. Ag and Sb contents are less than 0.1 wt%

Artefact	Cu (wt%)	Sn	Zn	Pb	Fe
Ca-C1	91.4	5.2	0.2	3.1	—
Ro-C3	91.0	6.5	—	2.3	0.2
AY-Sh4	87.2	10.4	1.2	0.6	0.5
Ro-N2	95.0	3.4	—	1.3	0.3

The surface chemical investigation of the *patina* grown on selected archaeological artefacts was carried out by using XPS analysis. All the patinas were characterised by the presence of cupric and/or cuprous compounds. As it is well known, these compounds under X-ray flux may be altered by the photoreduction effect induced by slow electrons generated by a non-monochromatized X-ray source and the reduction during Ar^+ ion sputtering. Because this effect varies the chemical nature of the copper species under investigation,[9,13] to avoid this problem, during the measurements, the samples were cooled with liquid N_2.[9]

Furthermore, for the XPS investigations to be performed, the Cu 2p, Cu LMM and valence band spectra for standard materials $Cu_2Cl(OH)_3$, $CuCl_2$, CuCl, Cu_2O and CuO were acquired, and the obtained results are listed in Table 2.

Figure 1 shows the data registered by the investigation of the first case of study, a Carthaginian coin labelled *Ca-C1* (third century BC) found at S. Antioco (Italy). The surface of this archaeological artefact is characterised by the presence of copper trihydroxychlorides [$Cu_2Cl(OH)_3$] polymorphs such as atacamite and paratacamite that reveal the occurrence of the self-sustaining process romantically defined 'bronze disease'. Such corrosive process disfigures and even destroys ancient objects. The typical aspect of these species that appear as a greenish powder on the surface of the archaeological bronzes is shown by the FE-SEM image, and the energy dispersive (ED) spectrum reveals the presence of oxygen, copper and chlorine. The Cu 2p photoemission signal shows the presence of strong shake-up satellites, characteristic for the copper in the oxidation state Cu^{2+}. Moreover, the value of the modified Auger parameter was 1851.4, typically assigned to Cu(II).[14] The BE value of the Cu $2p_{3/2}$ peak was 936.0 eV, and it can be assigned to atacamite [$Cu_2Cl(OH)_3$]. The depth profile, not reported for brevity, revealed that the chemical composition of the artefact remains constant even after a long time of sputtering and confirms a discrete amount of copper chloride species also in depth, where chlorine and copper are bonded to form nantokite (CuCl). Moreover, the elemental

Table 2. XPS result of the reference samples

Reference materials	Cu $2p_{3/2}$ (BE – eV)	Cu KLL (KE – eV)	α′
Cu (99.9%)	933.0	918.5	1851.5
Cu_2O	932.7	916.7	1849.4
CuO	934.0	917.5	1851.5
CuCl	932.7	915.6	1848.3
$CuCl_2$	935.2	915.4	1850.6
Archaeological Cu_2O	932.5	916.8	1849.3
Synthetic $Cu_2Cl(OH)_3$	935.2	916.6	1851.8

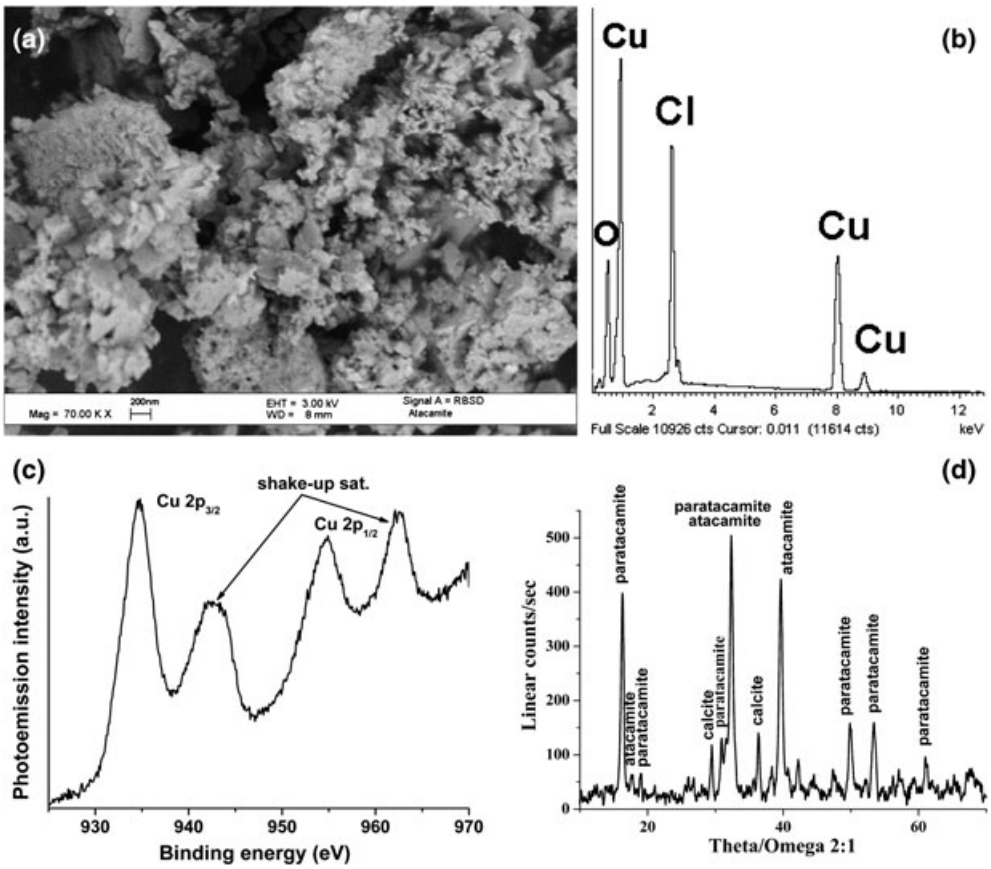

Figure 1. Field emission scanning electron microscope image (a) and energy dispersive spectrum (b) for the surface of the area where 'bronze disease' is occurring in the Carthaginian archaeological artefact (third century BC, label Ca-C1), X-ray photoelectron spectrum in the energy region of Cu 2p (c) and X-ray diffraction pattern (d).

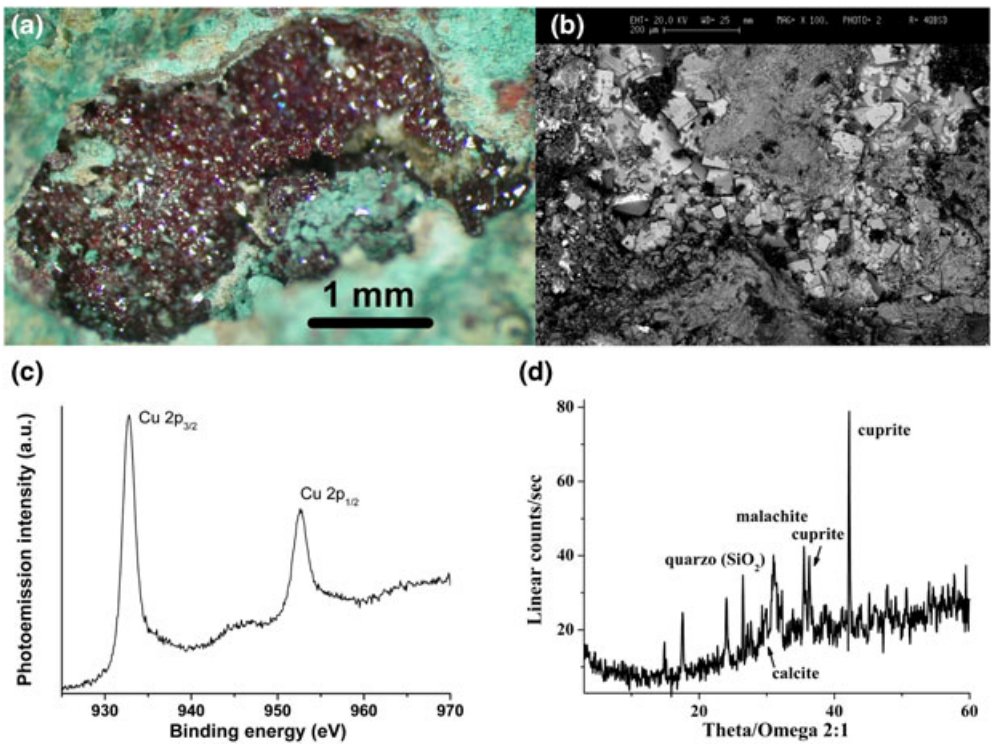

Figure 2. Optical microscopy and scanning electron microscopy images (a, b) for the surface of the area where cuprite (Cu2O) crystals are present mixed with a small amount of components of the soil and corrosion products grown on the surface of the Roman coin (first century BC, label Ro-C3), X-ray photoelectron spectrum in the energy region of Cu 2p (c) and X-ray diffraction pattern (d).

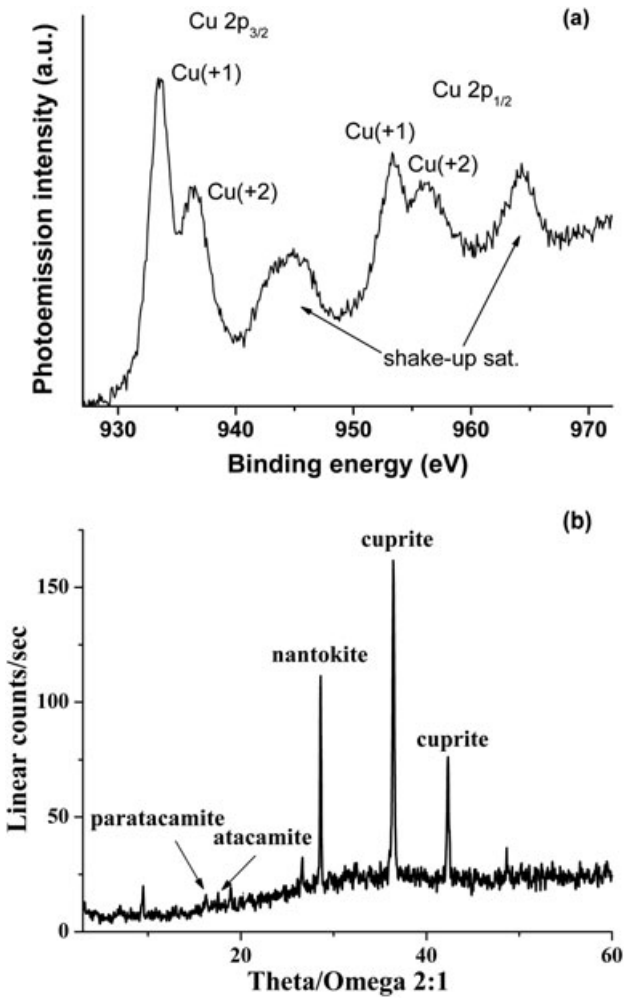

Figure 3. X-ray photoelectron spectrum in the energy region of Cu 2p (a) and X-ray diffraction pattern (b) for an area where nantokite (CuCl) is present on a Roman common use object (first century BC, label Ro-N2).

concentration depth profiles of the *Ca-C1* artefact reveal that Pb and Sn were not detected. This is probably due to the corrosion mechanism of Cu-based alloy in the presence of chloride ions that selectively attacks these elements, transforming them in soluble compounds during the long-term burial of the artefact as shown by accelerated electrochemical results.[15] It is worth noting that the formation of compounds between metal corrosion products and phosphorus or sulphur coming from the soil has not been detected by XPS, XRD and EDS techniques.[16,17]

The OM and SEM images (Fig. 2) display the surface of the Roman coin labelled *Ro-C3* (first century BC). In particular, the selected area shows the cuprite (Cu_2O) crystals mixed with a small amount of components of the soil and corrosion products. The presence of well-formed red-ruby cuprite crystals, revealed by OM image, was also confirmed by the XRD pattern that shows the occurrence of soil components such as quartz and calcite.

The Cu 2p signal displayed in Fig. 2 is characterised by a sharp Cu $2p_{3/2}$ peak positioned at BE = 933.5 eV. The BE value of Cu $2p_{3/2}$ and the value of the modified Auger parameter $\alpha' = KE(Cu\ LMM) + BE\ (Cu\ 2p_{3/2}) = 1848.2$ eV suggested that the oxidation state of Cu was +1. The detection of low intensity shake-up satellites localised at BE = 944.2 eV suggests the presence of Cu(II) because they can be considered as the fingerprint of Cu(II) compounds. This result was confirmed by XRD measurements that revealed also the presence of malachite. Concerning Sn and Pb, the lineshape analysis show that these element are present in a very low amount and in their oxidised state Sn^{4+} and Pb^{2+}.[18] The depth profile, not reported for brevity, revealed that the chemical composition of the artefact remains constant even after a long time of sputtering.

Figure 3 shows the X-ray photoelectron spectrum of the core level Cu 2p (on the left), and the XRD pattern acquired on a Roman common use object labelled *Ro-N2* (first century BC). The selected-area was characterised by the presence of nantokite (CuCl) and atacamite [$Cu_2Cl(OH)_3$]. In fact, the analysis of the Cu $2p_{3/2}$ peak revealed the presence of two contributions localised at BE = 933.5 and 936.5 eV, assigned to Cu(I) and Cu(II) oxidation states, respectively.

Figure 4 shows the OM image and the ED spectrum for the surface of a bronze shield labelled *AY-Sh4* (seventh century BC). The XRD measurements reveal the presence of copper carbonates such as malachite [$Cu_2(OH)_2CO_3$] and azurite [$Cu_3(OH)_2CO_3$] mixed[18] with a small amount of components of the soil and corrosion products as evidenced by ED spectrum and XPS elemental concentration depth profiles for Si, Ca, N, Sn, Cu, C and O. Silicates and carbonated were detected by XPS signals of Ca 2p, Si 2p and C 1s peaks positioned at BE = 347.7, 102.3 and 289.5 eV, respectively. In particular, a high amount of carbon was revealed because of the formation of copper carbonates, and also, nitrogen was detected likely due to soil contamination.

The Sn 3d signal was characterised by a Sn $3d_{5/2}$ peak localised at BE = 487.7 eV, assigned[19] to the oxidation state Sn^{+4}. Concerning copper, the peak fitting of Cu $2p_{3/2}$ signal (not shown) revealed a component positioned at BE = 936.2 eV, assigned to the oxidation state Cu(II) as also confirmed by the presence of the characteristic shake-up satellites, typical for Cu in oxidation state +2.

The obtained results confirmed the efficacy and versatility of the non-invasive or micro-destructive analytical techniques,[20] in particular, suggesting the need to select tailored conservation methods for these materials. However, according to our opinion, the best tailored strategies for long-term reliable conservation should be taken in consideration the transformation of dangerous copper chloride or oxy-chlorides into some stable phase to ensure a long-term chemical–physical stability of archaeological bronze artefacts.[21]

Conclusions

By means of the combined use of different analytical techniques such as XPS, SEM–EDS, MO and XRD, some exemplary *patinas* grown on of Roman and Punic archaeological bronze artefacts have been studied by selecting a suitable methodological approach to acquire detailed micro-chemical, morphological and structural information. The results provide good insight into the corrosion layers and evidence the presence of different species such as copper trihydroxychlorides $Cu_2Cl(OH)_3$, cuprite (Cu_2O), nantokite (CuCl), malachite [$Cu_2(OH)_2CO_3$] and azurite [$Cu_3(OH)_2CO_3$] mixed with soil components.

Finally, the obtained results showed that the combined study of XPS, SEM–EDS, XRD and OM analyses can be successfully used for the investigations of the corrosion products of archaeological copper-based objects to identify corrosion agents and mechanisms, suggesting the best reliable tailored strategies for the long-term reliable conservation of metal ancient artworks under uncontrolled atmosphere.

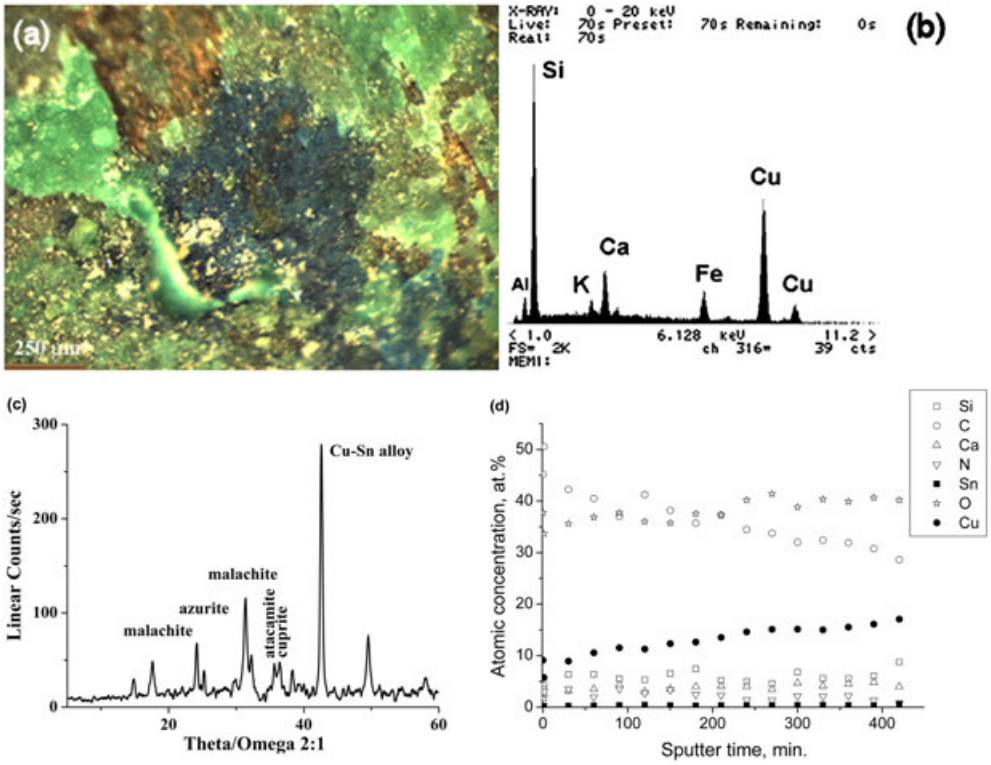

Figure 4. Optical microscopy image (a) and energy dispersive spectrum (b) for the surface of a bronze shield (seventh century BC, label AY-Sh4) where malachite [$Cu_2(OH)_2CO_3$] and azurite [$Cu_3(OH)_2CO_3$] crystals are present mixed with a small amount of components of the soil and corrosion products (first raw), X-ray diffraction pattern (c) and XPS elemental concentration depth profile (d).

Acknowledgements

This work has been financially supported by the European Commission (INCOMED contract n° ICA3-CT-2002-10030, acronym EFESTUS and INCOMED contract n° 509126, acronym PROMET) and by Italian MIUR (contract 2007PNA5ZT_005). The authors would express their sincere gratitude to the Soprintendenza Archeologica di Roma (Italy) and Cagliari ed Oristano (Italy) and to Claudio Veroli e Isabella Pierigè for useful discussions.

References

[1] D. J. Barber, I. C. Freestone. Archaeometry, **1990**, *32*, 33.
[2] G. M. Ingo, T. de Caro, C. Riccucci, E. Angelini, S. Grassini, S. Balbi, P. Bernardini, D. Salvi, L. Bousselmi, A. Çilingiroğlu, M. Gener, V. K. Gouda, O. Al Jarrah, S. Khosroff, Z. Mahdjoub, Z. Al Saad, W. El-Saddik, P. Vassiliou, *Appl. Phys. A*, **2006**, *83*, 513.
[3] M. Quaranta, I. Sandu, 9th International Conference on NDT of Art, Jerusalem Israel, 25–30 May **2008**.
[4] E. Mattson *et al.*, *The Central Board of National Antiquities and the National Historical Museums*, Stockholm, **1996**. ISBN 91-7209-014-6
[5] D. A. Scott, *Metallography and Microstructure of Ancient and Historic Metals*, The Getty Conservation Institute, The J. Paul Getty Museum. **1991**; p. 25.
[6] D. A. Scott, *J. Am. Inst. Conserv.* **1990**, *29*, 193.
[7] P. Lucey, *Britsh. Corros. J.* **1972**, *7*, 36.
[8] L. Robbiola, J. M. Blengino, C. Fiaud, *Corr. Sci. 1998*, 12, **2083**.
[9] R. Schlesinger, H. Klewe-Nebenius, M. Bruns, *Surf. Interf. Anal.* **2000**, *30*, 135.
[10] G. M. Ingo, G. Marletta, *Nucl. Instrum. Methods. Phys. Res. B* **1996**, *116*, 440.
[11] G. Cossu, G. M. Ingo, G. Mattogno, G. Padeletti, G. M. Proietti, *Appl. Surf. Sci.* **1992**, *56–58*, 81.
[12] D. Attanasio, G. Bultrini, G. M. Ingo, *Archa.* **2001**, *43*, 529.
[13] G. Panzner, B. Egert, H. P. Schmidt, *Suf. Sci.* **1985**, *151*, 400.
[14] J. F. Moulder, W. F. Stickle, P. E. Sobol, K. D. Bomben, Handbook of X-ray photoelectron spectroscopy, in *Physical Electronics* (Eds: J. Chastain, R. C. J. King), Physical electronics, Eden Praire, MN, **1995**.
[15] A. Carullo, F. Ferraris, M. Parvis, A. Vallan, E. Angelini, P. Spinelli, *IEEE T. Instrum. Meas.* **2000**, *49*, 371–375.
[16] C. Battistoni, M. P. Casaletto, G. M. Ingo, S. Kaciulis, G. Mattogno, L. Pandolfi, *Surf. Interface Anal.* **2000**, *29*, 773.
[17] G. M. Ingo, T. de Caro, C. Riccucci, S. Khosroff, *Appl. Phys. A* **2006**, *83*, 581–588.
[18] E. Angelini, P. Bianco, F. Rosalbino, M. Rosso, G. Scavino, *Werkst. Korros.-Matter. Corros.* **1994**, *45*, 392.
[19] G. M. Ingo, L. Giorgi, N. Zacchetti, N. Azzerri, *Corros. Sci.* **1992**, *33*, 361–377.
[20] G. M. Ingo, E. Angelini, G. Bultrini, T. De Caro, L. Pandolfi, A. Mezzi, *Surf. Interface Anal.* **2002**, *34*, 328.
[21] R. D'Agostino, F. Fracassi, F. Palumbo, E. Angelini, S. Grassini, F. Rosalbino, *Plasma Processes Polym.* **2005**, *2*, 91–96.

